



Performance Analysis of Optical Channel Multiplexing System on Indoor Light Fidelity (Li-Fi)

Fauza Khair¹ Fakhriy Hario^{2*} I Wayan Mustika³
 Sevia M. Idrus⁴ Anggun Fitriani Isnawati¹ Selo Sulisty³

¹Faculty of Telecommunication and Electrical Engineering, Institut Teknologi Telkom Purwokerto, Indonesia

²Department of Electrical Engineering, Faculty of Engineering, Universitas Brawijaya, Malang, Indonesia

³Department of Electrical and Information Technology, Universitas Gadjah Mada, Yogyakarta, Indonesia

⁴Faculty of Electrical Engineering, Universiti Teknologi Malaysia, 81310 Johor Bahru, Johor, Malaysia

* Corresponding author's Email: fakhriy08@ub.ac.id

Abstract: Li-Fi technology faces a critical challenge in achieving line-of-sight (LOS) connectivity while also optimizing bandwidth efficiency for high-speed data transmission. To address these issues, this research introduces a channel multiplexing model for Light Fidelity (Li-Fi) communication, employing movable LED panels. The study evaluates the model's performance by varying channel number, transmitter half-angle values, and field of view (FOV) parameters over a 3 to 5-meter transmission range. Results demonstrate that the proposed Light Fidelity indoor multiplexing model excels with an inter-channel spacing of 25 nm, particularly for Mux 2x2 and Mux 4x4 schemes. Longer-wavelength channels exhibit lower bit error rates (BER) and superior Q-factor values compared to others. Reliable performance within the 3 to 5-meter range is achieved with transmitter half-angle values of 30° and 45°, enhanced by adopting a higher Lambertian order value ($m > 1$) to ensure signal quality with a superior signal-to-noise ratio (SNR). Additionally, employing a FOV of 30° solely complies with the optical communication standard (BER < 10⁻¹²) for distances spanning 3 to 5 meters.

Keywords: Ber, Fov, Indoor li-fi, Multiplexing, Transmitter half angle.

1. Introduction

The increasing demand for high-speed communication technology has required advancements in telecommunications media, especially in wireless technology [1]. This technology faces challenges related to limited radio frequency spectrum allocation and reliance on high receiver sensitivity, despite its broad coverage at lower frequencies [1, 2]. Conversely, the increasing demand for capacity, coupled with the multifaceted correlation between environmental and security concerns, is a challenge for radio frequency communication technology [1, 2]. A potential solution to address this issue is optical wireless communication technology, which includes the utilization of light fidelity (Li-Fi) [1-4]. Li-Fi technology utilizes light as a medium for

transmitting information, adhering to the visible light communication (VLC) standard [4], which operates at a wavelength of 375 nm to 780 nm by following the IEEE 802.15.7 standard [5, 6]. Li-Fi has a wide range of applications, including smart rooms and smart cities, Internet of Things (IoT), communication connections in airplanes, patient monitoring, traffic control, disaster management, education or schools, and military [7–13]. Li-Fi technology is anticipated to emerge as an eco-friendly, more cost-effective alternative to wireless fidelity (Wi-Fi) technology [4], especially for indoor use [1].

Previous research has focused on the design and model of Li-Fi technology, achieving a significant increase in received signal quality through integrating optical amplifiers and filters [14]. Research [14] is only for system modeling for point

to point (PTP), while our proposed research applied the multiplexing for point to multi point (PTMP) system. In contrast, in signal transmission, the channel coding techniques and the orientation of light emission at the transmitter side have become the main parameters with a significant influence on the received signal quality [2, 3], [14-16]. These considerations are also relevant when examining the receiver side, where factors like the reception area size, field of view (FOV) value, reception angle orientation, and detector area demand thorough attention when modeling Li-Fi communications [3], [15], [17].

Another research [1] introduced a Li-Fi communication model that employed both fixed and movable LED Panels. The research comprehensively discussed the effects of wavelength variation and data rate, while also observing the model performance in relation to changes in the transmitter half angle and field of view (FOV). The test results indicated that the performance of all wavelength variations meets optical communication standards within a transmission distance range of up to 8 meters. The designed system model revealed that the utilization of both fixed and movable LEDs produced no substantial performance differences for wavelength variations between 450 nm and 650 nm. In addition, any increase in the transmitter angle by half LED to a significant rise in the bit error rate (BER) and a drastic decrease in the Q-factor. Research [1] is for fixed and movable systems, our proposed research is specifically for only movable systems.

Li-Fi technology offers wide bandwidth and high data rates, providing opportunities for enhancing both transmitter and receiver efficiency and capacity [18]. However, Li-Fi technology faces limitations in accurately positioning devices for line-of-sight (LOS) conditions, necessitating the use of multiplexing systems to boost bandwidth efficiency, especially in indoor settings [18, 19]. Research has proposed multiple input multiple output (MIMO) scenarios, with findings indicating that 2x2 and 4x4 channel multiplexing schemes result in nearly identical received power values. However, increasing the channel spacing value, from 5 nm to 25 nm, affects system performance, where the 25 nm channel spacing scenario demonstrates better performance [18], although reliable observation distance is still limited to 3 meters. Research [18] only reached a distance of 3 meters, our proposed research was made at a distance of 3-5 meters to see the quality of system modeling based on increasing transmission distance.

The research has also investigated the influence of half-angle values and field of view (FOV) on the Li-Fi multiplexing system model [19], showing that angle variations from 30° to 75° meet the standards, even though with a bit rate limit of 20 Mbps per channel and propagation distance of up to 3 meters. The research suggests the implementation of indoor Li-Fi multiplexing using a transmitter half-angle value and a small FOV.

Based on these factors, increasing bandwidth capacity and efficiency via a multiplexing system must consider a range of parameters linked to signal transmission at the transmitter end, channel propagation characteristics, and reception factors at the receiver side.

In order to provide a thorough assessment of the effectiveness of the suggested multiplexing channel model, this study will take into account the transmitter specifications, FOV values, and number of channels as well as transmitter half-angle values and transmitter half-angle values as well as signal transmission propagation parameters. The research will focus on indoor Li-Fi and will measure the maximum transmission range at a transmission distance of 3 to 5 meters.

The remaining sections of this paper are structured as follows: Section 2 explains the system blocks of the proposed Li-Fi indoor multiplexing model, presents the mathematical formulations for each sub-system, and specifies the testing parameters. Following this, Section 3 presents the results for each observation scenario, conducting a performance analysis based on the number of channels, transmitter half angle value, and FOV value in Li-Fi indoor multiplexing evaluated with a 20 Mbps bit rate per channel using simulation. Lastly, Section 4 offers a concise summary of the key findings.

2. Proposed model of multiplexing channel system on indoor light fidelity (Li-Fi)

This research proposes a multiplexing system model employing multiple channels, using a movable LED panel scheme for indoor Li-Fi propagation. The utilization of movable LED panels on the indoor Li-Fi aligns with established standards and, as a result, does not yield any significant difference compared to fixed LED panels. Generally, the proposed system consists of three basic blocks: the optical modulation and LED multiplexing blocks on the Li-Fi transmitter side, the Li-Fi indoor transmission media channel, and the demultiplexing and optical detection blocks on the receiver side.

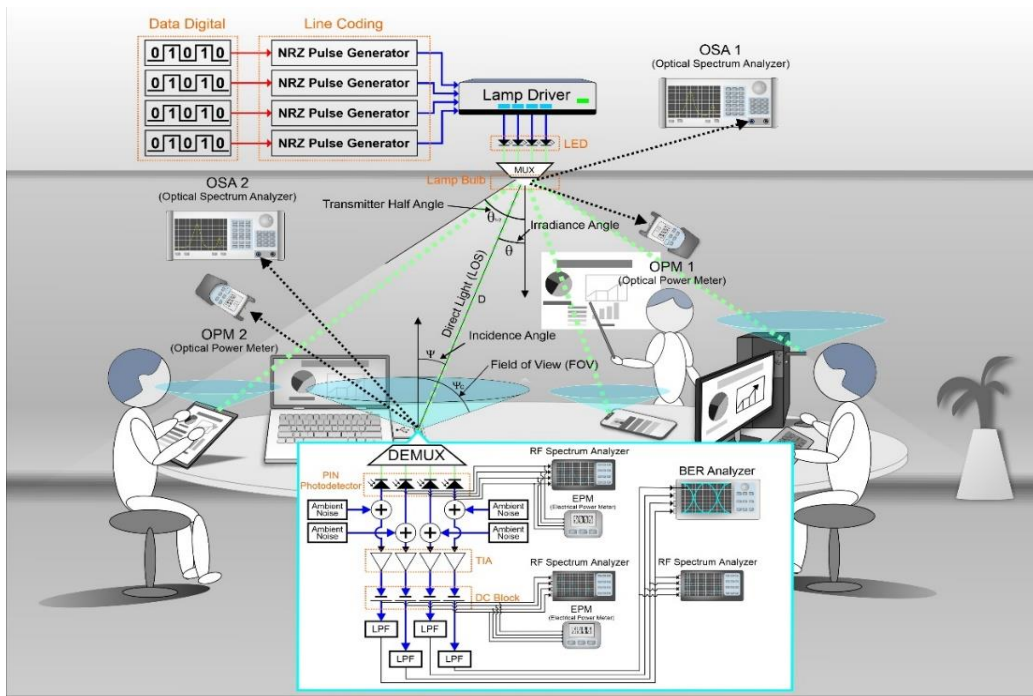


Figure. 1 The Proposed Model of Multiplexing Channel System on Indoor Light Fidelity (Li-Fi)

The assessment of the proposed model involves a thorough examination of the effects of altering the number of channels for multiplexing, specifically focusing on 2x2 and 4x4 channels. Additionally, this study also investigates the model’s performance based on varying the transmitter half-angle value and FOV value, while maintaining a data rate of 20 Mbps for each channel. The proposed model block system visualization is shown in Figure 1.

In this multiplexing system, the communication process begins with transmitting digital data from the Li-Fi transmitter system block. These bit sequences are generated based on a 20 Mbps data-rate using a pseudo-random bit sequence generator (PRBS). Subsequently, the digital data undergoes non-return to zero (NRZ) line coding generation, resulting in electrical data with the specified data-rate. Following this, the data is then directed to the up-conversion system for the electrical-to-optical (E/O) modulation.

The proposed model uses the optical direct modulated LED (DML) scheme, using an optical source from the lamp driver. The LED multiplexing scheme operates within the wavelength range from 430 nm to 505 nm, with a channel bandwidth of 0.03 nm for each channel. Regarding the up-conversion process on the transmitter side, the conversion of current into optical power is influenced by the LED’s responsiveness (P), which is directly proportional to the frequency value (f) and quantum efficiency (η) value of each LED. The

LED responsiveness of each channel can be calculated using formula (1) [1]:

$$P = \eta \cdot h \cdot f \cdot \frac{i(t)}{q} \quad (1)$$

where q is the electron charge, h is the plank constant, and $i(t)$ is the modulation current signal. Thus, by employing a multiplexing system involving several LED channels, the total LED responsiveness value is obtained, formulated as follows [18, 19].

$$P_{mux} = \eta_s \cdot h \cdot f_{tot} \cdot \frac{i(t)_{tot}}{q_{tot}} \quad (2)$$

Formula (1) serves to assess the up-conversion characteristics of the DML, drawing on the current transfer function that is linked to the electron lifetime parameter τ_n and the product of circuit resistance and circuit capacitance τ_{rc} of the LED device. The current transfer function can be formulated as [1]:

$$H(f) = \frac{1}{1 + j2\pi f(\tau_n + \tau_{rc})} \quad (3)$$

The increase in bandwidth resulting from the introduction of the proposed multiplexing system for both the mux two and mux four channel schemes is

proportional to the increase in the number of channels as formulated by formula (4). The quantum efficiency percentage value can be determined using formula (5) [18, 19].

$$B_{tot}(nm) = B_1 + B_2 + \dots + B_n \quad (4)$$

$$\eta_s(\%) = \left(\frac{B_{tot}}{\Delta v} \right) \times 100\% \quad (5)$$

where Δv is the channel spacing range (nm).

By referring to formula (2), the current transfer of a 2-channel multiplexing system can be formulated as follows [18, 19].

$$H(f)_{mux(2ch)} = H(f_1) + H(f_2) \quad (6)$$

$$H(f)_{mux(2ch)} = \frac{1}{1 + j2\pi \cdot f_1(\tau_n + \tau_{RC})} + \frac{1}{1 + j2\pi \cdot f_2(\tau_n + \tau_{RC})} \quad (7)$$

Therefore, the calculation of the total current transfer value is:

$$H(f)_{mux(2ch)} = \frac{1 + j2\pi \cdot f_1(\tau_n + \tau_{RC}) + 1 + j2\pi \cdot f_2(\tau_n + \tau_{RC})}{(1 + j2\pi \cdot f_1(\tau_n + \tau_{RC})) \cdot (1 + j2\pi \cdot f_2(\tau_n + \tau_{RC}))} \quad (8)$$

$$H(f)_{mux(2ch)} = \frac{2 + j2\pi(f_1 + f_2)(\tau_n + \tau_{RC})}{1 + j2\pi(f_1 + f_2)(\tau_n + \tau_{RC}) - 4\pi^2 f_1^2 f_2^2 (\tau_n + \tau_{RC})^2} \quad (9)$$

$$H(f)_{mux(2ch)} = \frac{2 + j2\pi(f_1 + f_2)(\tau_n + \tau_{RC})}{(2\pi f_1 f_2)^2 \cdot (\tau_n + \tau_{RC})^2} \quad (10)$$

Based on the same calculation concept as formula (6), the current transfer value for modeling a 4-channel multiplexing system can be formulated as follows.

$$H(f)_{mux(4ch)} = H(f_1) + H(f_2) + H(f_3) + H(f_4) \quad (11)$$

$$H(f)_{mux(4ch)} = \frac{1}{1 + j2\pi \cdot f_1(\tau_n + \tau_{RC})} + \frac{1}{1 + j2\pi \cdot f_2(\tau_n + \tau_{RC})} + \frac{1}{1 + j2\pi \cdot f_3(\tau_n + \tau_{RC})} + \frac{1}{1 + j2\pi \cdot f_4(\tau_n + \tau_{RC})} \quad (12)$$

The light emitted from the LED lamp driver following the multiplexing of various wavelengths conforms to the Lambertian cosine law, resembling radiation patterns. This radiation represents emitted or reflected light flux, called Lambertian radian intensity, where the light flux received is calculated as a unit solid angle per unit area. The value of the Lambertian flux intensity, which depends on the radiation angle (θ) and Lambertian order (m) value, can be determined using the following formula [1], [14], [18], [19]:

$$R_0 = \left(\frac{m+1}{2\pi} \right) \cos^m \theta \quad (13)$$

The Lambertian order (m) is calculated using formula (14), where variable $\theta_{1/2}$ is the transmitter half-angle value [1], [14].

$$m = - \left(\frac{\ln 2}{\ln(\cos \theta_{1/2})} \right) \quad (14)$$

This research evaluates the performance of the Li-Fi indoor multiplexing system by varying transmitter half-angle values within the range of 30° to 75° at a line of sight (LOS) propagation distance spanning from 3 to 5 meters. The LED emission pattern emits symmetrical radiation, meaning that the radiation amount is directly proportional to the product of the LED's emitting power and the Lambertian flux intensity. The Li-Fi receiver modem receives this radiation from the connection, and these signals are subsequently converted into electrical signals by a photodetector. The proposed detection system model uses direct detection with a certain reception angle. Based on formula (13), the power value per received area, expressed in W/cm^2 , can be calculated using the following formula [1], [14], [19]:

$$I_s[d, \theta] = \frac{P_t \times R_0(\theta)}{d^2} \quad (15)$$

here, d is the distance between the transmitter and the receiver. Considering the effective detector area (A_{eff}) in relation to the receiving structure, the received power (P_r) is determined as follows [1], [14], [18]:

$$P_r = I_s[d, \theta] \times A_{eff}(\psi) \quad (16)$$

where A_{eff} can be calculated using formula (14) [14]:

$$A_{eff}(\psi) = \begin{cases} A_{det} T_s(\psi) g(\psi) \cos(\psi) & 0 \leq \psi \leq \psi_c \\ 0 & \psi > \psi_c \end{cases} \quad (17)$$

Based on formula (17), the A_{eff} value depends on detector area (A_{det}), lens gain (g), filter transmission gain (T_s), ψ_c field of view (FOV), and angle of incidence (ψ). The calculation of lens gain is formulated as follows (18) [14], [20-22]:

$$g(\psi) = \begin{cases} \frac{n^2}{\sin^2 \psi_c} & 0 \leq \psi \leq \psi_c \\ 0 & \text{otherwise} \end{cases} \quad (18)$$

where n is the refractive index of the concentrator. The first reflection of DC channel gain $H(0)_{LOS}$ in the LOS transmission can be formulated as follows [14], [21], [23]:

$$H(0)_{LOS} = \begin{cases} \frac{(m+1)A}{2\pi d^2} \cos^m(\theta) T_s(\psi) g(\psi) \cos(\psi) & 0 \leq \psi \leq \psi_c \\ 0 & \psi > \psi_c \end{cases} \quad (19)$$

By substituting formula (16), the value of receiving power can be formulated into formula (17) [1], [14], [21].

$$P_r = \begin{cases} \frac{P_t(m+1)A_{det}}{2\pi d^2 \sin^2 \psi_c \cos^m(\theta)_s (\psi)^2 \cos(\psi)} & 0 \leq \psi \leq \psi_c \\ 0 & \psi > \psi_c \end{cases} \quad (20)$$

The optical signal spectrum received by the receiver undergoes a down-conversion process using a direct detection scheme by a photodetector. The signal spectrum results from demultiplexing performed by the optical mux to achieve a signal with the same frequency and channel spacing as the transmitter. Any pulse widening caused by an increase in the transmit angle, signal linewidth, or the reception area of the light sensor due to an expansion of the FOV can be mitigated through a filtering process utilizing an optical rectangle filter. Subsequently, the output from each photodetector undergoes electrical reinforcement facilitated by a DC block and trans-impedance amplifier (TIA). The amplified signal also goes through an electrical filtering process to anticipate and address any noise, using a low pass filter (LPF) with a transfer function formulated by formula (21) with an insertion loss value α of 0 dB and a depth (D) of 100 dB. The cut-off frequency of LPF is set at $0.75 \times \text{bit rate}$ [1]:

$$H(f) = \begin{cases} \alpha, (f_c - B/2 < f < f_c + B/2) \\ d \end{cases} \quad (21)$$

where B is the bandwidth parameter (Hz), while f is the signal frequency (Hz). The general parameters used for performance observing the proposed Li-Fi indoor multiplexing model are shown in Table 1.

3. Result and discussion

3.1 Multiplexing 2x2 channel and 4x4 channel

Observations were carried out to analyze the performance of the proposed model, primarily focused on increasing the number of multiple channels, specifically, mux 2x2 and mux 4x4, starting from a distance of 3 to 4 meters.

Table 1. General Parameter of Multiplexing Indoor Li-Fi

Parameter	Value
Bit rate	20 Mbps per Channel
LED wavelength	430 nm – 505 nm (Blue LED)
Channel Spacing	5 up to 25 nm
Channel bandwidth	0.03 nm
Distance	3 up to 5 m
Detector Area	1.5 cm ²
FOV	30 ⁰ up to 75 ⁰
Index Concentrator	1.5
Transmitter Half Angle	30 ⁰ up to 75 ⁰
Irradiance Angle	20 ⁰
Incidence Angle	20 ⁰
PIN Responsivity	0.1 A/W
Detector Sensitivity	-28 dBm
Cut Off Frequency	0.75*bit rate (Hz)

Table 2. Channel Wavelength Specification

Chan-nel Spacing (nm)	Mux 2x2		Mux 4x4			
	Ch-1 (nm)	Ch-2 (nm)	Ch-1 (nm)	Ch-2 (nm)	Ch-3 (nm)	Ch-4 (nm)
5	430	435	430	435	440	445
10	430	440	430	440	450	460
15	430	445	430	445	460	475
20	430	450	430	450	470	490
25	430	455	430	455	480	505

Table 3. Lambertian Order and Flux Intensity Calculation.

$\theta_{1/2}$	m	R_0
30 ⁰	4.819	8.585
45 ⁰	2.000	4.426
60 ⁰	1.000	2.951
75 ⁰	0.513	2.232

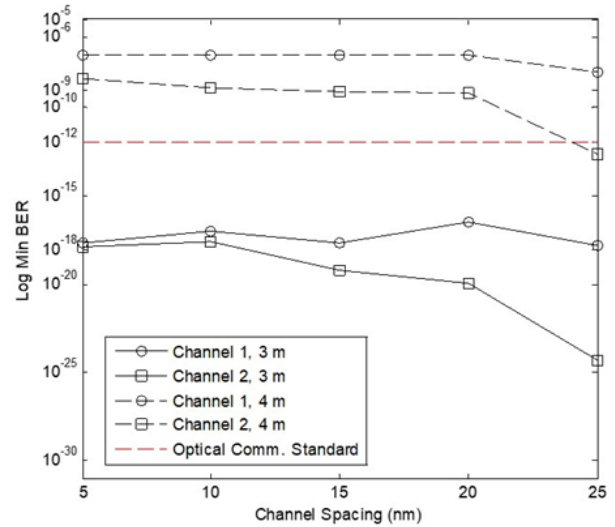
Furthermore, the influence of channel spacing, from 5 to 25 nm, was considered to assess the reliability of frequency allocation, as shown in Table 2. This experiment was limited to scenarios with an FOV value of 600 and a value of $m=1$ or when the transmitter half angle value was set at 600, as calculated using formulas (13) and (14) in Table 3.

Based on the observed results for Mux 2x2, as shown in Figure 2 (a), the BER value decreased as the spacing between channels increased. This decrease in BER value can be attributed to the smaller interference effect between channels. However, the BER value that meets optical communication standards (below 10^{-12}) can only be achieved at a distance of 3 meters. Meanwhile, at a distance of 4 meters, in general, the BER value obtained exceeds 10^{-12} . Even with a channel spacing of 25 nm, the BER value obtained by Channel 2 (455 nm) is 2.46×10^{-13} . Figure 2 (a) also illustrates that the BER value for Channel 2 is smaller than that of Channel 1 (430 nm). This phenomenon occurs because the spectral response and emission at the 455 nm wavelength are remarkably higher [1], [5].

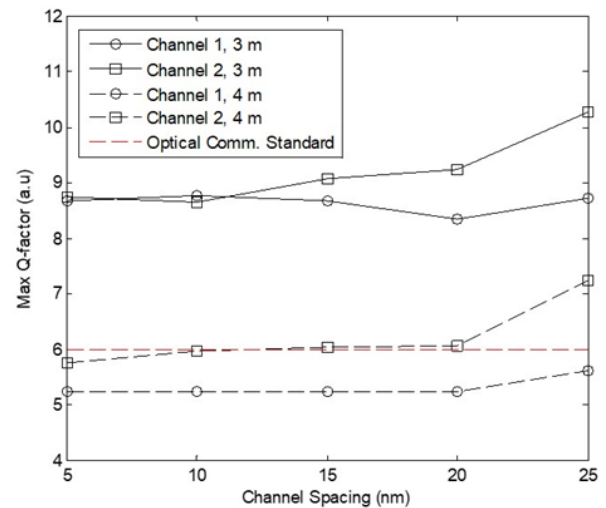
An increase in the Q-factor value was also obtained due to the wider channel spacing. At a distance of 3 meters, the Q-factor value was more than 9 arbitrary units, as shown in Figure 2 (b). However, at a distance of 4 meters, despite Channel 2 (455 nm) continuing to meet optical communication standards (threshold 6 a.u.) with channel spacing ranging from 10 to 25 nm, the Q-factor value of Channel 1 (430 nm) was below 5.5 a.u. This outcome is comparable to the BER value presented in Figure 2 (a).

Consequently, the use of 25 nm channel spacing is recommended for this Li-Fi multiplexing model to ensure compliance with the available bandwidth allocation on the blue LED.

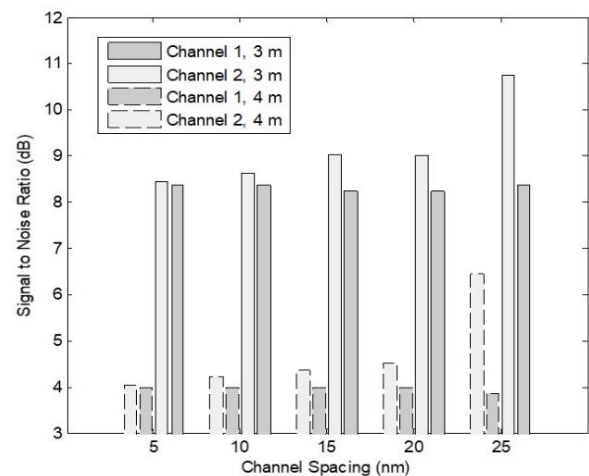
The decrease in the BER value and the increase in the Q-factor value were proportional to the SNR value obtained, as illustrated in Figure 2 (c). At a distance of 3 meters, the SNR value for both channels 1 and 2 exceeded 8 dB. The trend of increasing SNR values is notable, reaching up to 11 dB for Channel 2 when using a 25-nm channel spacing. However, Channel 1 does not follow this trend; maintaining a consistent relative SNR value is 8 dB across all channel spacing variations. When extending the transmission distance to 4 meters, Channel 2 only achieved an SNR value of 6.5 dB at a channel spacing of 25 nm. Even with channel spacings between 5 to 20 nm, both Channel 1 and Channel 2 yielded SNR values in the range of 4 to 5



(a)



(b)



(c)

Figure 2 Results for Mux 2 channels on distances of 3 m and 4 m: (a) Min. BER, (b) Max. Q-factor, and (c) SNR

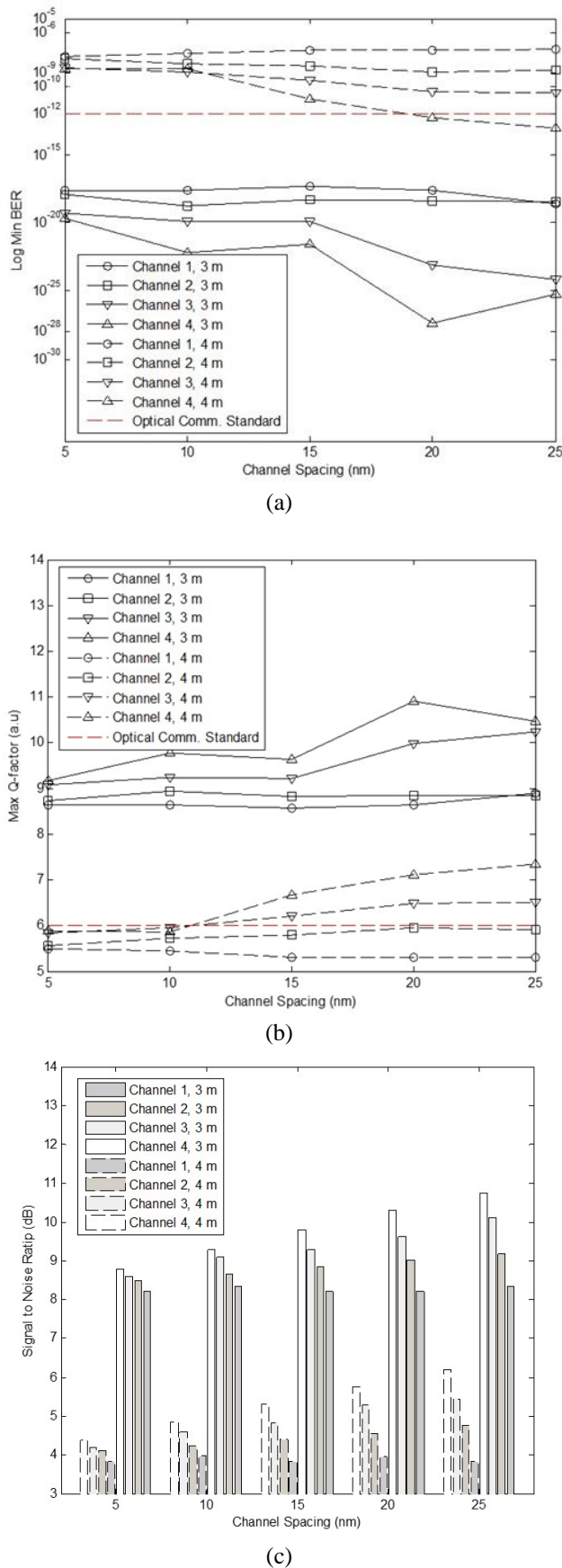


Figure 3 Results for Mux 4 channels on distances of 3 m and 4 m: (a) Min. BER, (b) Max. Q-factor, and (c) SNR

dB. These results signify the need to enhance the responsiveness of the PIN photodetector used and consider using a more sensitive filter to anticipate existing noise.

To assess the results obtained in the two-channel multiplexing, the Mux 4x4 system was observed. The main objective of this test was to evaluate the impact of increasing the number of channels alongside the increase in channel spacing on the overall performance of the Li-Fi multiplexing model, as shown in Figure 3.

According to the results of the BER values presented in Figure 3 (a), at a distance of 3 meters, all channels exhibited a BER value of less than 10^{-18} . Similar to the Mux 2x2 findings, these results also indicate that using a larger wavelength yields the smallest BER values, observed in Channel 3 and Channel 4. Using channel spacing of 20 nm and 25 nm is recommended for Mux 4x4, as it results in BER values below 10^{-23} .

The proposed multiplexing model is in line with the standard requirements set by the available bandwidth allocation. However, when extending the LOS transmission distance to 4 meters, all channels failed to meet the minimum BER requirements for - channel spacing variations of 5 nm to 15 nm. For channel spacing of 20 nm and 25 nm, only Channel 4 had a BER value below 10^{-12} . Therefore, the proposed multiplexing model, Mux 4x4, can increase the bandwidth up to fourfold according to formula (4), although it is only limited to a distance of 3 meters.

Meanwhile, the Q-factor value results, as shown in Figure 2 (b), revealed that at a transmission distance of 3 meters, all channels within Mux 4x4 exhibited Q-factor values ranging from 8.5 a.u. to 11 a.u. Unlike the previous BER results, Channel 3 and Channel 4, with 20 and 25 nm channel spacing, still maintained a Q-factor value exceeding the standard (6 a.u.). These findings suggest that the proposed multiplexing model can accommodate an increased number of channels, provided that the channel spacing is limited to 20 nm.

The increase in SNR value is also comparable to the use of 4x4 multiplexing. At a distance of 3 meters, the highest SNR value is obtained on Channel 4, reaching up to 11 dB, as shown in Figure 3 (c). The increase in the number of channels, with channel spacing between 5 nm and 25 nm, affects the SNR value for each channel. Channel 1 remained in the range of 8 dB, whereas Channel 2 rose to 9 dB. A significant surge was observed in Channels 3 and 4, ranging from 8.8 dB to 11 dB. However, the SNR decreased when extending the transmission distance to 4 meters, with all channels

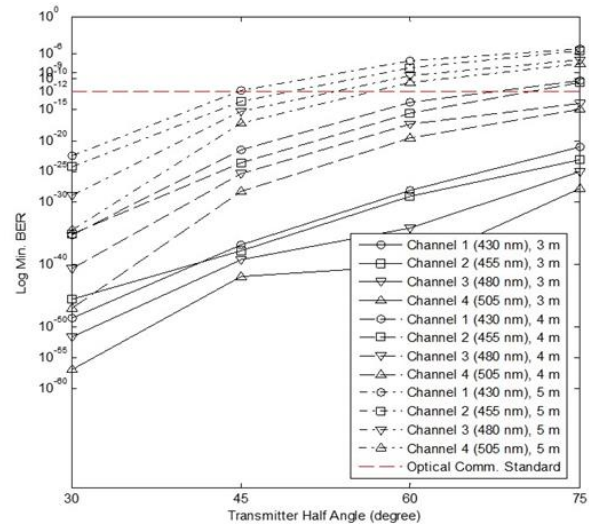
displaying an SNR value below 6 dB. Therefore, based on these results, it is necessary to consider enhancing the detector’s sensitivity and applying appropriate gain to increase the signal power level.

3.2 Transmitter half angle variation for Mux 4x4 channels

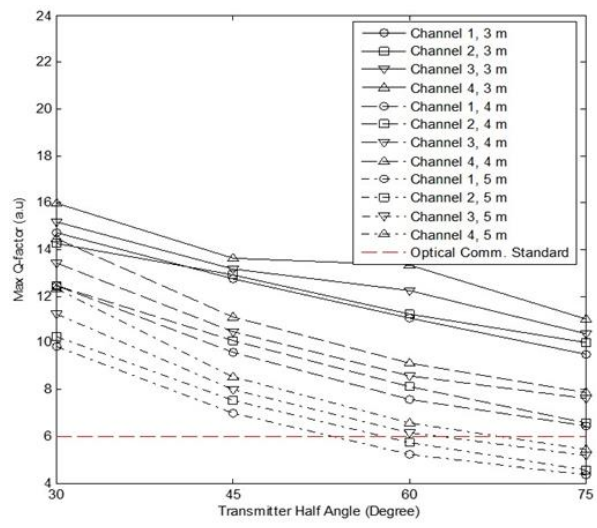
Meanwhile, at a distance of 5 meters, the BER values obtained for all channels exceeded the error of 10^{-12} . A similar trend was observed when using a value of 75° , where the performance obtained remained suitable for a distance of 3 meters. However, at a distance of 4 meters, only channels 3 and 4 were still good. At a distance of 5 meters, the BER values for all channels were notably elevated. These results validate the reliability of the proposed multiplexing system model within the 3 to 5-meter range, particularly when the transmitter’s half-angle values were set at 30° and 45° . Considering the data rate remains at 20 Mbps per channel, this result represents an opportunity to increase the bandwidth. However, it is crucial to consider several acceptance parameters, such as FOV and A_{eff} , as formulated by formulas (17) and (18).

Meanwhile, a similar trend was observed in the Q-factor results when considering varying transmitter half-angle values, as shown in Figure 4 (b). In this case, the Q-factor value that meets the standard is the same as the previous BER findings. For a transmitter half-angle value of 30° , exceptionally high Q-factor values, exceeding 10 a.u., are achieved up to a 5-meter distance. Even at a 3-meter distance, all channels exhibit Q-factor values surpassing 14 a.u. Similar results were observed for the 45° , where the system performance was still above standard (greater than 6 a.u.) up to a distance of 5 meters. However, different results were yielded for the values 60° and 75° , where the system could only meet the requirements up to a distance of 4 meters. Consequently, these results recommend the use of a smaller transmitter half-angle value.

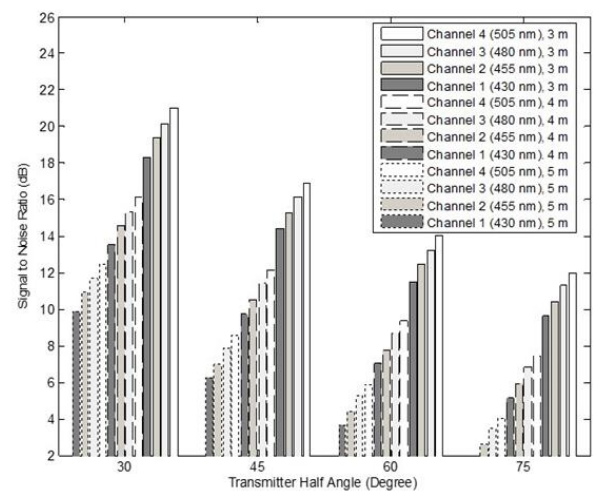
Similar results were shown in the SNR values obtained for each variation in the observed transmitter half-angle value, as shown in Figure 4 (c). The increase in SNR value applies to the increase in channel wavelength usage, where Channel 4 had the highest SNR. At a distance of 3 meters, Channel 4 achieved an SNR value of 21 dB when employing a 30° transmitter half-angle. However, this value decreased with an increase in the transmitter half-angle value, where Channel 4



(a)



(b)



(c)

Figure. 4 Results for transmitter half angle variation on distances of 3 m up to 5 m: (a) Min. BER, (b) Max. Q-factor, and (c) SNR

had an SNR value of 12 dB at an angle of 75° . In general, the decline in SNR value ranges from 4 to 6 dB as the distance increases from 3 meters to 5 meters for all channels. Based on these results, increasing the transmitter half-angle value significantly reduces the signal power of the received signal. Therefore, based on the SNR parameter, it is recommended to use a smaller transmitter half-angle value.

3.3 FOV variation for Mux 4x4 channels

The subsequent observation is the performance of the proposed Li-Fi indoor multiplexing model, based on the influence of FOV variations ranging from 30° to 75° . The mathematical formulation refers to formulas (17-20), with FOV's influence extending to the fluctuating values of A_{eff} , H_{LOS} , and received power P_r . Similar to the previous research, the transmitter half angle was limited when $m=1$ or 60° with irradiance angle and incidence values of 20° for the movable LED panel scheme. The data rate was maintained at 20 Mbps per channel, with a 4x4 Mux multiplexing system test. The results measuring the performance of the proposed model under the influence of FOV value variations are shown in Figure 5.

As illustrated in Figure 5 (a), BER value results meeting the optical communication standard are observed for distance variations of 3 meters to 5 meters, particularly when the FOV value is 30° , where the BER values obtained range from 10^{-45} to 10^{-55} for all Mux 4x4 channels at distance 3 meters. Moreover, at a distance of 3 and 4 meters, utilizing an FOV value of 45° , all channels still reached a BER value below 10^{-12} . However, under these conditions, none of the channels received a BER value below 10^{-12} at a distance of 5 meters. Different results were obtained when values of 60° and 75° were applied, where the performance of the proposed model was only reliable for a distance of 3 meters.

At distances of 4 meters and 5 meters, this configuration is no longer suitable. Thus, it can be concluded that there is a proportional increase in BER values as the FOV value increases, with an average standard deviation of 1.925×10^{-5} at 3 meters, 1.05×10^{-9} at 4 meters, and 1.793×10^{-5} at 5 meters. These elevated error values suggest that employing an FOV of 30° is highly recommended for this multiplexing model system.

The Q-factor results mirror the BER value, as shown in Figure 5 (b). At FOV 30° , all channels exhibit Q-factor values above the standard, ranging from 9 a.u. to 16 a.u. Even though Channels 3 and 4

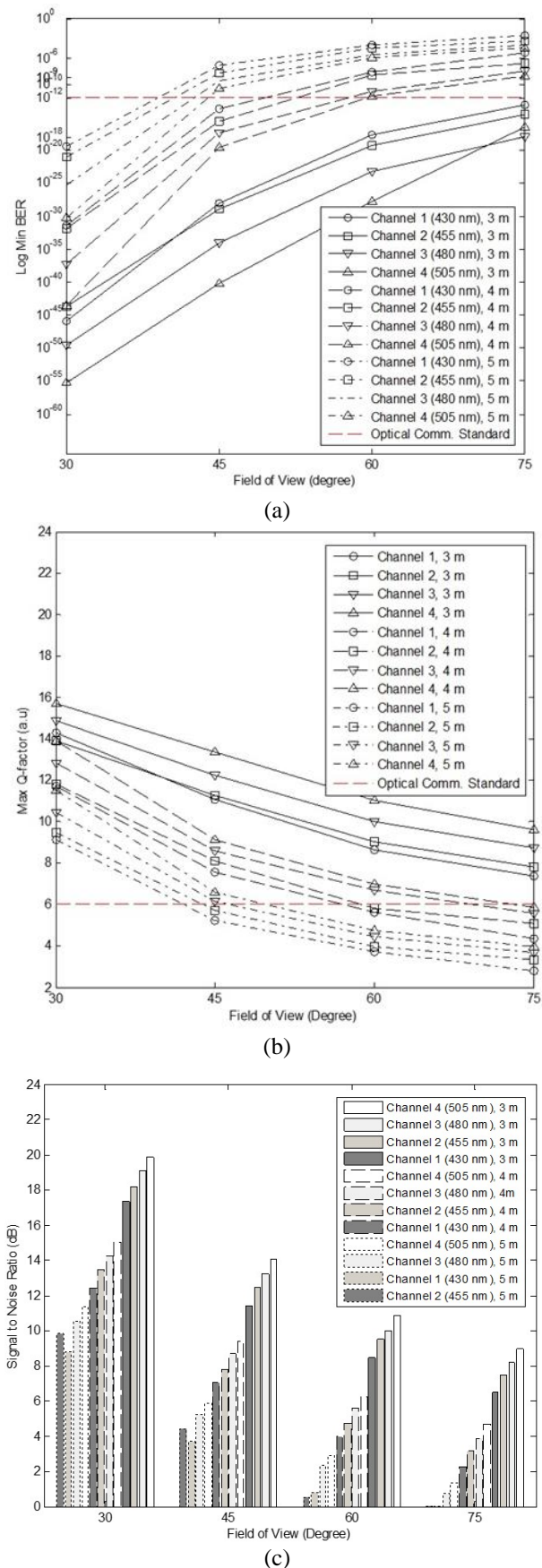


Figure 5 Results for FOV variation on distances of 3 m up to 5 m: (a) Min. BER, (b) Max. Q-factor, and (c) SNR

maintain a Q-factor value above 6 at a distance of 5 meters, FOV 45° only meets the performance target at 3 and 4 meters for all channels. The decrease in the Q-factor value tends to be significant in proportion to the increased FOV angle. Based on formula (17), the HLOS value is null when the FOV is smaller than the incidence angle. Using an incidence angle value of 20° and FOV variations ranging from 30° to 75° shows that the HLOS value plays a role in determining the reflection of DC channel gain. Therefore, the incidence angle selection must be taken into consideration to determine the appropriate FOV for providing an appropriate gain for the signal reception process. Based on the findings, the recommended FOV value for this model is between 30° and 45° .

The increase in gain value, as formulated by formula (18) due to the utilization of a smaller FOV, also significantly affects the SNR value obtained, as shown in Figure 5 (c). This result is closely related to the received power outlined in formula (20). Observing the downward trend in SNR, it is evident that system performance will decrease when utilizing a larger FOV, specifically 60° and 75° . As a result, the SNR value significantly drops to levels below 4 dB. This phenomenon also causes system performance to decrease, as evidenced in performance evaluations based on the number of multiplexing channels, as shown in Figure 2 and Figure 3 when employing an FOV of 60° . Consequently, the results highlight the importance of adopting a smaller FOV and a lower incidence angle value for the proposed model.

4. Conclusion

Based on the test results, the proposed Light Fidelity indoor multiplexing model exhibits optimal performance with an inter-channel spacing of 25 nm, whether in Mux 2x2 and Mux 4x4 schemes. These results indicate that channels with longer wavelengths have lower BER values and higher Q-factor values than other channels. The proposed multiplexing model proves reliable for distances ranging from 3 to 5 meters, with recommended half-angle transmitter values of 30° and 45° . Furthermore, employing a higher Lambertian order value ($m > 1$) guarantees reception signal quality with a higher SNR. Additionally, using a FOV of 30° is the sole configuration capable of meeting the optical communication standard ($BER < 10^{-12}$) for a distance of 3 to 5 meters. The test results also suggest opportunities for increasing the number of channels for multiplexing systems at distances of 3 meters and 4 meters, as well as the possibility of increasing

the bit rate for the Mux 4x4 scheme at a distance of 3 meters with transmitter half-angle values of 30° and FOV 30° .

Conflicts of Interest

The authors declare no competing interests relevant to this content article. The datasets generated during and analyzed during the current research are available from the corresponding author.

Author Contributions

F.H., F.K., and I.W.M. initiated the research topic, proposed the main ideas, and designed the model. F.K., I.W.M., and S.M.I. developed the mathematical model and layout simulation and extracted the results. A.F.I. and S.S. contributed to the results analysis. All authors collaborated on writing and reviewing the manuscript.

Acknowledgments

This study has been partially funded by the Ministry of Education, Culture, Research and Technology of the Republic of Indonesia. Additionally, this study received support from the Electronics System Laboratory of Gadjah Mada University, the Telecommunication Laboratory of Universitas Brawijaya, and the Optical & Photonic Laboratory of Institut Teknologi Telkom Purwokerto, as well as the Lightwave Communication Research Group in the Faculty of Electrical Engineering, Universiti Teknologi Malaysia.

References

- [1] F. Khair, W. Mustika, D. Zulherman, and F. Hario, "Performance Analysis of Indoor Light Fidelity Technology Propagation Using Fixed and Movable LED Panels", *Int. J. Intell. Eng. Syst.*, Vol. 16, No. 2, pp. 1–13, 2023, doi: 10.22266/ijies2023.0430.01.
- [2] T. C. Bui, S. Kiravittaya, K. Sripimanwat, and N. H. Nguyen, "A comprehensive lighting configuration for efficient indoor visible light communication networks", *Int. J. Opt.*, Vol. 2016, 1–9, 2016.
- [3] F. Aftab, M. N. U. Khan, and S. Ali, "Light fidelity (Li-Fi) based indoor communication system", *Int. J. Comput. Netw. Commun.*, Vol. 8, No. 3, pp. 21–31, 2016.
- [4] F. Aftab, "Potentials and challenges of light fidelity based indoor communication system", *Int. J. New Comput. Archit. their Appl.*, Vol. 6, No. 3, pp. 91–102, 2016.

- [5] L. M. Matheus, A. B. Vieira, L. F. M. Vieira, M. A. M. Vieira, and O. Gnawali, "Visible light communication: concepts, applications and challenges", *IEEE Commun. Surv. Tutorials*, Vol. 21, No. 4, pp. 3204–3237, 2019.
- [6] V. Swetha and E. Annadevi, "Survey on light-fidelity", In: *Proc. of International Conference on Smart Systems and Inventive Technology (ICSSIT 2018)*, pp. 355–358, 2018.
- [7] D. B. Kuttan, S. Kaur, B. Goyal, and A. Dogra, "Light Fidelity: A future of wireless communication", In: *Proc. of 2021 2nd Int. Conf. Smart Electron. Commun. ICOSEC*, pp. 308–312, 2021.
- [8] M. S. Chandra, S. Saleem, S. L. Harish, R. Baskar, and P. C. Kishoreraja, "Survey on Li-Fi technology and its applications", *Int. J. Pharm. Technol.*, Vol. 8, No. 4, pp. 20116–20123, 2016.
- [9] V. V. Andreev, "Wireless technologies of information transmission based on the using of modulated optical radiation (Li-Fi communication system): State and prospects", In: *Proc. of 2018 Syst. Signal Synchronization, Gener. Process. Telecommun. SYNCHROINFO*, Vol. 2018, pp. 1–4, 2018.
- [10] P. Kuppusamy, S. Muthuraj, and S. Gopinath, "Survey and challenges of Li-Fi with comparison of Wi-Fi", In: *Proc. of 2016 IEEE Int. Conf. Wirel. Commun. Signal Process. Networking, WiSPNET 2016*, pp. 896–899, 2016.
- [11] T. A. Nugraha and Y. Ardiyanto, "Li-Fi Technology for Transmitting Data in Hospital Environments", In: *Proc. of 1st Int. Conf. Inf. Technol. Adv. Mech. Electr. Eng. ICITAMEE 2020*, Vol. 0, pp. 81–84, 2020.
- [12] J. I. Janjua, T. A. Khan, M. S. Khan, and M. Nadeem, "Li-Fi communications in smart cities for truly connected vehicles", In: *Proc. of 2nd 2021 Int. Conf. Smart Cities, Autom. Intell. Comput. Syst. ICON-SONICS 2021*, pp. 1–6, 2021.
- [13] M. F. Tota, "Light Fidelity (Li-Fi) Communication Applied to Telepresence Robotics", In: *Proc. of IEEE 21th International Carpathian Control Conference (ICCC)*, Vol. 59, p. 978, 2020, doi: 10.1109/ICCC49264.2020.9257292.
- [14] S. Razzaq, N. Mubeen, and F. Qamar, "Design and analysis of light fidelity network for indoor wireless connectivity", *IEEE Access*, Vol. 9, pp. 145699–145709, 2021.
- [15] H. D. Huynh and K. S. Sandrasegaran, "Coverage performance of light fidelity (Li-Fi) network", In: *Proc. of 2019 25th Asia Pac. Conf. Commun. APCC 2019*, pp. 361–366, 2019.
- [16] S. K. Yaklaf and K. S. Tarmissi, "Multi-carrier modulation techniques for light fidelity technology", In: *Proc. of 19th Int. Conf. Sci. Tech. Autom. Control Comput. Eng. STA 2019*, pp. 70–73, 2019.
- [17] H. D. Huynh, K. Sandrasegaran, and S. C. Lam, "Modelling and simulation of handover in light fidelity (Li-Fi) network", In: *IEEE Reg. 10 Annu. Int. Conf. Proc. TENCON*, pp. 1307–1312, 2019.
- [18] I. W. Mustika, F. Khair, A. F. Isnawati, T. A. Dewi, D. E. Setyawan, and A. A. F. Purnama, "Modeling of Multiplexing Indoor Light Fidelity (Li-Fi) Technology Using Movable LED Panel", In: *Proc. of IEEE Int. Conf. Commun. Networks Satell. COMNETSAT 2022*, pp. 14–20, 2022, doi: 10.1109/COMNETSAT56033.2022.9994385
- [19] I. W. Mustika, F. Khair, A. F. Isnawati, A. N. Aini Maryadi, D. E. Setyawan, and A. A. Faradila Purnama, "Analysis of Transmitter Half Angle and FOV Variations on Multiplexing Indoor Li-Fi Communication", In: *Proc. of IEEE Int. Conf. Commun. Networks Satell. COMNETSAT 2022*, Vol. 201, No. Vlc, pp. 444–450,
- [20] A. Raza, H. Mehdi, Z. Hussain, and S. Hussain, "Visible Light Communication (Li-Fi Technology)", In: *Proc. of IEEE 2021 International Conference on Computing, Electronic and Electrical Engineering (ICE Cube)*, 2021. doi: 10.1109/ICECube53880.2021.9628334.
- [21] R. Riaz, S. S. Rizvi, F. Riaz, S. Shokat, and N. A. Mughal, "Designing of cell coverage in Light Fidelity", *Int. J. Adv. Comput. Sci. Appl.*, Vol. 9, No. 3, pp. 44–53, 2018.
- [22] R. Ghahramani Negar Sendani, "Study the effect of FOV in visible light communication", *Int. Res. J. Eng. Technol.*, Vol. 04, No. 10, pp. 759–763, 2017.
- [23] C. Chen, I. Tavakkolnia, M. D. Soltani, M. Safari, and H. Haas, "Hybrid multiplexing in OFDM-based VLC systems", In: *Proc. of 2020 IEEE Wirel. Commun. Netw. Conf. WCNC*, pp. 1–6, 2020.